Nonlinear Robust Voltage Regulation and Balanced Demand Response of an Islanded DC Microgrid

Sajed Derakhshani Pour
Department of Electrical Engineering
Sahand University of Technology
Tabriz, Iran
s_derakhshanipour99@sut.ac.ir

Reza Eslami
Department of Electrical Engineering
Sahand University of Technology
Tabriz, Iran
eslami@sut.ac.ir

Mousa Marzband
Department of Mathematics, Physics and Electrical Engineering
Northumbria University
Newcastle, England
mousa.marzband@northumbria.ac.uk

Sajjad Shoja-Majidabad
Department of Electrical Engineering
University of Bonab
Bonab, Iran
shoja.sajjad@ubonab.ac.ir

***Abstract*—Robust voltage regulation and balanced demand response of the islanded DC microgrids (MGs) in the presence of variable loads and different solar irradiations have gained increasing interest in recent years. To achieve these objectives, a nonlinear robust cascaded voltage controller comprised of proportional integral (PI) and sliding mode control (SMC) methods is proposed for the battery energy storage system (BESS) in this paper. A backstepping sliding mode control (BSMC) is also investigated for maximum power point tracking (MPPT) of the solar array. The efficient performance of the proposed nonlinear control approach is analyzed by MATLAB/Simulink. The simulation results demonstrate robust voltage regulation of DC bus with minor tracking error and fast response against load demand and irradiance variations in addition to ensuring the balanced demand response of DC MG.**

Keywords—DC Microgrid, Nonlinear robust voltage regulation, Maximum power point tracking, Battery energy storage system

I. INTRODUCTION

A. Motivations

Traditional energy sources like fossil fuels are the world's chief sources of energy. Consumption of these sources offers a wide range of drawbacks such as an increase in the amount of the greenhouse gases and pollution, decreased resource reservation results in intense energy crises, financial problems and infirm system performance. Renewable energy sources (RESs) like widely utilized solar photovoltaic (PV) systems are replacing those of traditional energy sources in order to tackle the abovementioned problems. However, the intermittent nature of RESs impels them to be integrated with BESSs as MGs to preserve the power stability between generation side and demand side [1-3]. MGs fall within DC and AC types. DC MGs present more advantages as compared to AC MGs such as elimination of frequency and reactive power parameters, greater and more accurate system performance, high reliability and low environmental pollutions [4]. Fig. 1 demonstrates the proposed DC MG structure. In this configuration, the PV array is connected to the DC link by a DC-DC boost converter, while BESS is linked to the DC bus through a DC-DC bidirectional converter.

B. Literature Review

Robust voltage regulation and balanced demand response of the islanded PV/BESS DC MGs in the presence of variable loads and supply variations have attracted the attention of scholars in the last few years. Therefore, a wide variety of control approaches such as single PI, droop control, SMC and model predictive control (MPC) are introduced for MGs in literature. In [5], a simple PI-based control strategy is proposed for a DC MG with a hybrid energy storage system to reach voltage control and equal power sharing. In [6], the effective function of PV/Fuel Cell/Storage/Hydrogen AC MG is verified by PI controller. In [7,8], adaptive droop control strategies are proposed for DC MG in order to cope with voltage control and balanced current distribution. In [9], SMC is presented to preserve the output voltage level of islanded PV/Battery DC MG. An integrated SMC is designed and compared with single PI control in [10] to demonstrate the performance improvement of DC MG. In [11], a decentralized model predictive control (DMPC) is recommended to guarantee the voltage control and power distribution of DC MG with constant power loads (CPLs).

C. Gaps and Contributions

Given the above, several gaps have been recognized in the existing literature as follows:

1) In [5,6], PI controllers are linear while power electronic systems are mostly nonlinear. In addition, the control performance of single PI controllers will be downgraded toward abrupt variations in the operating condition of DC MG due to the fact that the PI controller suffers from severe sensitivity against uncertainties.
2) In droop control strategies [7,8], voltage control may be disturbed due to equal current sharing that causes a voltage drop. Thus, balanced power sharing among RESs and proper voltage regulation will not be available anymore.
3) However, SMC approach in [9,10] offers robust and fast performance against uncertainties, suffering from chattering problem that causes possible steady-state errors.
4) In [11], MPC method require high computational time and cost to carry out owing to the high uncertainties of the system model. Furthermore, MPC needs the exact dynamic model of the system.

The contributions and objectives of this paper are introduced in the following based on the abovementioned gaps:

- A nonlinear robust controller composed of PI and SMC controllers is proposed for PV/Storage DC MG to achieve DC bus voltage maintenance and balanced demand response under various load demands and solar irradiations.
- A BSMC is proposed on the basis of the maximum power point (MPP) to extract the peak power from the solar PV.
- Compared to other control approaches, the leading characteristics of the proposed control strategy are less DC bus voltage fluctuations, more robust performance, faster dynamic response and reduced chattering effects.

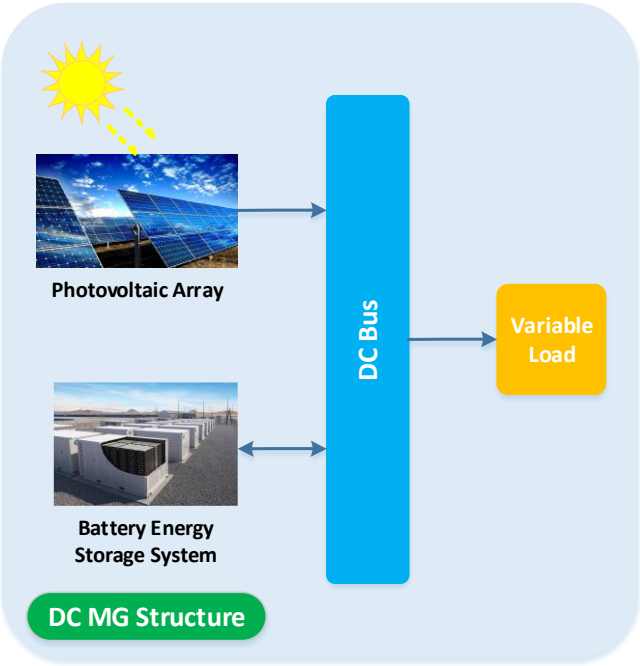

Fig. 1. The proposed islanded DC microgrid

D. Paper Organization

The rest of the paper is arranged as follows: Section II describes the proposed DC MG model. In Section III, formulations of the proposed model control approach are presented. Section IV illustrates the simulation results and case studies. Eventually, section V ends the paper.

II. Model Description

A. PV Array

As one of the best alternatives for DC MG power supply, solar PV systems emit zero carbon and reduce electricity generation costs. Solar irradiation and cell temperature directly affect the PV output power. In this structure, the solar panel is linked to DC bus by a DC-DC boost converter in order to supply the load. Solar PV array should work at the peak point of the P-V curve to generate the maximum possible power. Thus, the MPP-based BSMC is exploited here to track the peak point. The considered PV module is KC200GH-2P with 54 series-connected cells, the electrical parameters of which are presented in Table I.

B. Battery Energy Storage System

In order to control power disparity between generation and demand, the BESS is linked to the DC bus via a bidirectional DC-DC converter. The proposed PI-SMC controller maintains the healthy operation of DC MG by charging and discharging the BESS in the following states:

- Charging mode: The excessive power is stored in the BESS in this scenario because the requested output power is lower than the generated power by solar PV.
- Discharging mode: Under this condition, the PV array cannot fully respond to the requested load power. Thus, the battery will be discharged to compensate the required load power.

TABLE I. PV Module Electrical Parameters

Parameter	Value
MPP voltage V_{mpp}	26.6 [V]
MPP current I_{mpp}	7.55 [A]
Maximum power P_{mpp}	200 [W]
Short circuit current I_{sc}	8.21 [A]
Open circuit voltage V_{oc}	32.9 [V]
Temperature coefficient of short circuit current K_{sc}	0.00479
P-N junction ideality factor n	1.8
Cell temperature T	25 [℃]

III. Control Startegy Formulation

A. MPPT Control

To obtain the maximum possible output from the PV system, the MPP-based BSMC consisting of two control loops is developed. By taking advantage of PV voltage and PV current, the MPP block evaluates the peak point and provides the MPP voltage used as a reference in the second loop [2]. In the second loop, BSMC produce the control signal by receiving the PV voltage, PV current, MPP voltage or reference PV voltage, Inductor current, and output voltage as exposed in Fig. 2.

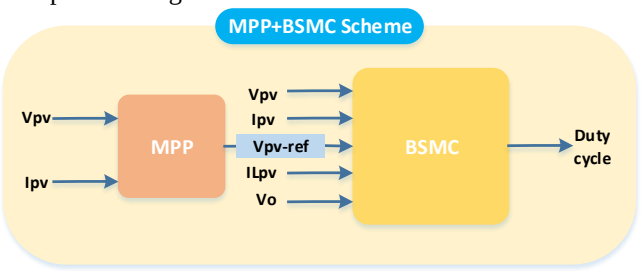

Fig. 2. MPPT controller

$$I_{pv} = N_p\left(I_{ph} - I_{sat}\left[\exp\left(\frac{V_{pv}}{\alpha N_s}\right) - 1\right]\right) \quad (1)$$

where N_p and N_s demonstrate the number of cells connected in parallel and in series respectively, I_{pv} is PV current and V_{pv} displayes PV voltage, and α is defined as a constant in the following:

$$\alpha = \frac{nTk_B}{q} \quad (2)$$

where $q = 1.6 \times 10^{-19}$ is the magnitude of electrical charge on the electron, n is the P-N junction ideality factor, $k_B = 1.3805 \times 10^{-23}$ represents the Boltzmann constant and T indicates the cell temperature.

$$I_{sat} = I_{satr}\left(\frac{T}{T_r}\right)^3 \exp\left(\frac{E_g T}{\alpha}\left[\frac{1}{T_r} - \frac{1}{T}\right]\right) \quad (3)$$

where I_{sat} is reverse bias saturation current of the cell, $E_g = 1.1$ is the energy gap of semiconductor and I_{satr} is reverse bias saturation current at reference temperature T_r which is given as follows:

$$I_{satr} = \frac{I_{sc}}{\exp\left(\frac{V_{oc}}{\alpha N_s}\right) - 1} \quad (4)$$

where I_{sc} and V_{oc} symbolize the short circuit current and the open circuit voltage respectively.

The photocurrent I_{ph} is dependant on the cell temperature and solar irradiation by:

$$I_{ph} = 0.001E[I_{sc} + K_{sc}(T - T_r)] \quad (5)$$

where E and K_{sc} depict the solar irradiation and the temperature coefficient of short circuit current respectively.

Therefore, PV power P_{pv} can be achieved in the following by taking (1) into consideration:

$$P_{pv} = V_{pv}I_{pv} = V_{pv}N_p\left(I_{ph} - I_{sat}\left[\exp\left(\frac{V_{pv}}{\alpha N_s}\right) - 1\right]\right) \quad (6)$$

Also, DC-DC boost converter equations of PV module are given by:

$$\begin{cases} \frac{dV_{pv}}{dt} = \frac{I_{pv}}{C_1} - \frac{I_{L-pv}}{C_1} \\ \frac{dI_{L_{pv}}}{dt} = f_1(x) + g_1(x)u_{pv} \\ \frac{dV_o}{dt} = f_2(x) + g_2(x)u_{pv} \end{cases} \quad (7)$$

where,

$$\begin{cases} f_1(x) = \frac{1}{L_{pv}}\left[V_{pv} + V_D - \frac{RR_c}{R+R_c}I_{L-pv} - \left(\frac{R_c}{R+R_c} - 1\right)V_o\right] \\ g_1(x) = \frac{1}{L_{pv}}\left[V_D + \frac{RR_c}{R+R_c}I_{L-pv} - \left(\frac{R_c}{R+R_c} - 1\right)V_o\right] \\ f_2(x) = \frac{1}{C}\left[\frac{R}{R+R_c}I_{L-pv} + \frac{1}{R+R_c}V_o\right] \\ g_2(x) = -\frac{R}{C(R+R_c)}I_{L-pv} \end{cases} \quad (8)$$

In the equations above, I_{L-pv} and V_o are the PV inductor current and DC MG output voltage respectively, L_{pv} is PV inductance, C is DC link capacitor, $V_D = 0.82$ illustrates the voltage across the diode, R is the amount of the output load and R_c equals 39.6 Ω.

In order to generate the reference PV voltage or MPP voltage, the MPP block is designed by the following equation:

$$\frac{dP_{pv}}{dI_{pv}} = \frac{d(V_{pv}I_{pv})}{dI_{pv}} = V_{pv} + I_{pv}\frac{dV_{pv}}{dI_{pv}} = 0 \quad (9)$$

Based on (8) in view of (1), the PV voltage V_{pv} is obtained as follows:

$$V_{pv} = \alpha N_s \log\left(\frac{I_{sat} + I_{ph} - I_{pv}}{I_{sat}}\right) \quad (10)$$

Derivative of PV voltage V_{pv} with respect to PV current I_{pv} gives:

$$\frac{dV_{pv}}{dI_{pv}} = -\alpha N_s\left(\frac{1}{I_{sat} + I_{ph} - I_{pv}}\right) \quad (11)$$

Replacing (9) and (10) in (8), the following equation is obtained:

$$\log\left(\frac{I_{sat} + I_{ph} - I_{pv}}{I_{sat}}\right) = \frac{1}{I_{sat} + I_{ph} - I_{pv}} \quad (12)$$

The subsequent equation indicates a correlation between the desired maximum power current I_d and the photocurrent I_{ph}.

$$I_d = 0.91I_{ph} \quad (13)$$

Finally, the required PV reference voltage or MPP voltage is generated [2] by replacing I_d instead of I_{pv} in (9).

$$V_{pv-ref} = \alpha N_s \log\left(\frac{I_{sat} + 0.091I_{ph}}{I_{sat}}\right) \quad (14)$$

The BSMC controller should compel the PV voltage V_{pv} to track the reference PV voltage V_{pv-ref} in order to obtain the maximum power.

The tracking errors are introduced as follows:

$$\begin{cases} e_1 = V_{pv} - V_{pv-ref} \\ e_2 = I_{L-pv} - I_{L-pv-ref} \end{cases} \quad (15)$$

where $I_{L-pv-ref}$ is the reference current that will be explained later.

In the first step, the time derivative of e_1 in view of (7) is given by:

$$\dot{e}_1 = \frac{I_{pv}}{C_1} - \frac{I_{L-pv}}{C_1} - \dot{V}_{pv-ref} \quad (16)$$

The above equation can be rewritten as

$$\dot{e}_1 = \frac{I_{pv}}{C_1} - \frac{e_2}{C_1} - \frac{I_{L-pv-ref}}{C_1} - \dot{V}_{pv-ref} \quad (17)$$

To stabilize (17), the following virtual control is proposed:

$$I_{L-pv-ref} = C_1\left(\frac{I_{pv}}{C_1} - \dot{V}_{pv-ref} - M_1e_1 - M_{1sw}sign(e_1)\right) \quad (18)$$

where $M_1 > 0$ and $M_{1sw} > 0$ are the controller gains. Now, by selecting the Lyapunov function $V_1 = \frac{1}{2}e_1^2$, one finds

$$\dot{V}_1 = e_1\dot{e}_1 = e_1\left(\frac{I_{pv}}{C_1} - \frac{e_2}{C_1} - \frac{I_{L-pv-ref}}{C_1} - \dot{V}_{pv-ref}\right)$$

$$= e_1\left(-\frac{e_2}{C_1} - M_1e_1 - M_{1sw}sign(e_1)\right)$$

$$= -\frac{e_1 e_2}{C_1} - M_1 e_1^2 - M_{1sw}|e_1| \quad (19)$$

In the second step, by differentiating from $e_2 = I_{L-pv} - I_{L-pv-ref}$, one obtains

$$\dot{e}_2 = \dot{I}_{L-pv} - \dot{I}_{L-pv-ref}$$
$$= f_1(x) + g_1(x)u_{pv} - \dot{I}_{L-pv-ref} \quad (20)$$

In order to stabilized (20), the Lyapunov candidate function is chosen as follows:

$$V_2 = V_1 + \frac{1}{2}e_2^2 \quad (21)$$

By taking time derivative and substituting (19), one finds

$$\dot{V}_2 = -\frac{e_1 e_2}{C_1} - M_1 e_1^2 - M_{1sw}|e_1| + e_2\dot{e}_2$$
$$= -\frac{e_1 e_2}{C_1} - M_1 e_1^2 - M_{1sw}|e_1|$$
$$+e_2\left(f_1(x) + g_1(x)u_{pv} - \dot{I}_{L-pv-ref}\right) \quad (22)$$

Thus, the following control law is proposed:

$$u_{pv} = \frac{1}{g_1(x)}\left(-f_1(x) + \dot{I}_{L-pv-ref} + \frac{e_1}{C_1} - M_2 e_2 - M_{2sw} sign(e_2)\right) \quad (23)$$

where $M_2 > 0$ and $M_{2sw} > 0$ are the controller gains. The rest of proof can be found in [12].

B. PI-SMC voltage control

To guarantee the robust voltage regulation and balanced demand response of DC MG, the PI-SMC controller is proposed as shown in Fig. 3. The PI controller generates the reference battery current I_{b-ref} for SMC by receiving the difference between the output load voltage V_o and its reference value V_{o-ref} and the SMC acquires the battery current I_b, the output voltage V_o and the reference battery current I_{b-ref} in order to preserve the DC bus voltage at the desired level in addition to control the power sharing among PV array and BESS to supply the variable load.

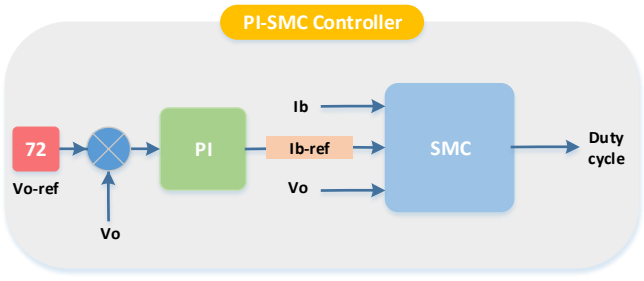

Fig. 3. PI-SMC voltage controller

$$\begin{cases} \frac{dV_o}{dt} = \frac{1}{C}(1-u_b)I_b + d_0(t) \\ \frac{dI_b}{dt} = -(1-u_b)\frac{V_o}{L_b} + \frac{V_b}{L_b} + d_b(t) \end{cases} \quad (24)$$

where V_o and V_b are the output load voltage and the battery voltage respectively, C is DC link capacitor, I_b is battery current, L_b is battery inductance, and $d_0(t)$ and $d_b(t)$ are the uncertainty terms which assumed to be limited to:

$$\begin{cases} |d_0(t)| \le \Delta_0 \\ |d_b(t)| \le \Delta_b \end{cases} \quad (25)$$

where Δ_0 and Δ_b are known positive constants.

Introducing the tracking errors as follows:

$$\begin{cases} e_o = V_o - V_{o-ref} \\ e_b = I_b - I_{b-ref} \end{cases} \quad (26)$$

The following PI controller is utilized to produce the reference battery current for the SMC block.

$$I_{b-ref} = K_3 e_o + K_4 \int e_o dt \quad (27)$$

where K_3 and K_4 symbolize proportional and integral parameters.

Time derivative of e_b in view of (18) is given as follows:

$$\dot{e}_b = \dot{I}_b - \dot{I}_{b-ref}$$
$$= -(1-u_b)\frac{V_o}{L_b} + \frac{V_b}{L_b} + d_b(t) - \dot{I}_{b-ref} \quad (28)$$

Finally, the succeeding SMC principle is proposed to generate the voltage tracking control signal u_b:

$$u_b = 1 - \frac{L_b}{V_o}\left(\frac{V_b}{L_b} - \dot{I}_{b-ref} + K_b e_b + K_{b-sg} sgn(e_b)\right) \quad (29)$$

where K_b is the battery control gain and K_{b-sg} displays the sliding gain.

C. Stability proof

Taking the succeeding Lyapunov function into consideration:

$$V_{total} = V_2 + V_b = V_1 + \frac{1}{2}e^2 + V_b \quad (30)$$

By taking derivative of (30) as follows:

$$\dot{V}_{total} = e_1\dot{e}_1 + k_1 e_1^2 - k_1 e_1^2 + e_b\dot{e}_b - S\dot{S}$$
$$\le -e_1^2 - e_b^2 - \delta S^2 - \beta|S| \quad (31)$$

where δ and β are positive values. Thus, $\dot{V}_{total}$ will be negative.

IV. Case Studies and Simulation Results

The considered islanded DC MG is simulated in the MATLAB/Simulink to indicate the healthy operation of the proposed control method. Specifications of DC MG are presented in Table II. In the beginning, the MPP-based BSMC approach is proposed for the PV array DC-DC boost converter to obtain the maximum power. To achieve this goal, PV output voltage V_{pv} well tracks its reference value or MPP voltage V_{pv-ref} quickly as exposed in Fig. 4(a). The reference voltage

of the PV array equals 26.6 V. Therefore, the maximum extracted power reaches 200 W in irradiance of 1000 W/m^2 and temperature of 25℃ as shown in Fig. 7. Also, the amount of irradiance varies rapidly from 1000 W/m^2 to 500 W/m^2 at $t = 10 - 12\ s$ and the maximum extracted power reduces to 100 W in this condition. Fig. 4(b) points out the PV current, which is around 7.55 A.

TABLE II. DC MG PARAMETERS

Parameter	Value
DC link capacitor C	1000 [μF]
PV capacitor C_1	1000 [μF]
PV inductance L_{pv}	1.21 [mH]
Battery inductance L_b	3.3 [mH]
Switching frequency	5000 [Hz]
Load powers P_o	300 [W], 200 [W], 100 [W]
Variable resistive load values R	17.28 [Ω], 25.92 [Ω], 51.84 [Ω]

Next, the PI-SMC controller is proposed for bidirectional DC-DC converter to achieve robust DC bus voltage control and balanced demand response. $K_3 = 0.001$ and $K_4 = 10$ represent the PI parameters. In order to represent the capability of the proposed controller, several step changes in load demand and solar irradiation are implemented as exposed in Fig. 5(a) and Fig. 5(b) respectively. The load demand variation directly corresponds to the requested load power and irradiance change affects the produced PV power. In other words, the requested load power is increased with a decrease in the resistive load and decreased with an increase in it. and PV generation is reduced with a decline in solar irradiation. All these changes in supply and demand sides are able to increase the DC link voltage tracking error e_o and demolish the voltage stability. Fig. 6(a) depicts the ability of the proposed nonlinear robust controller in maintaining the DC bus voltage level at its desired value of 72 V with low fluctuations and fast speed in the presence of different load demands and irradiances. Fig. 6(b) displays the output load current, which is varied by the mentioned step changes. Furthermore, the balanced demand response among PV array and BESS to provide the required load demand is achieved as displayed in Fig. 7 based on the following case studies. It is worth mentioning that P_{pv}, P_b and P_o illustrate PV generated power, battery output power and output load power respectively in this figure.

A. *Case 1: Demand Increment (2<t<4)*

The resistive load is reduced to 17.28 Ω and the required load power is increased to 300 W in this period. So, BESS must switch to discharging mode in order to meet the needed output load power due to the fact that the supplied PV power is not sufficient.

B. *Case 2: Demand Decrement (6<t<8)*

The required load power is decreased to 100 W in this interval due to an increase of the resistive load to 51.84 Ω. Thus, the produced PV output provides the required power demand and the surplus power is stored in BESS.

C. *Case 3: No Demand Change*

As long as the requested output power is equal to the generated PV power at 200 W, then there is no need to the commitment of BESS and it only meets MG losses. The resistive load value is 25.92 Ω in this case.

D. *Case 4: Irradiance Decrement (10<t<12)*

Solar irradiation is decreased to 500 W/m^2 in this time period. Therefore, the generated PV power is reduced to about 100W and BESS will immediately switch to discharging mode in order to supply the required load power.

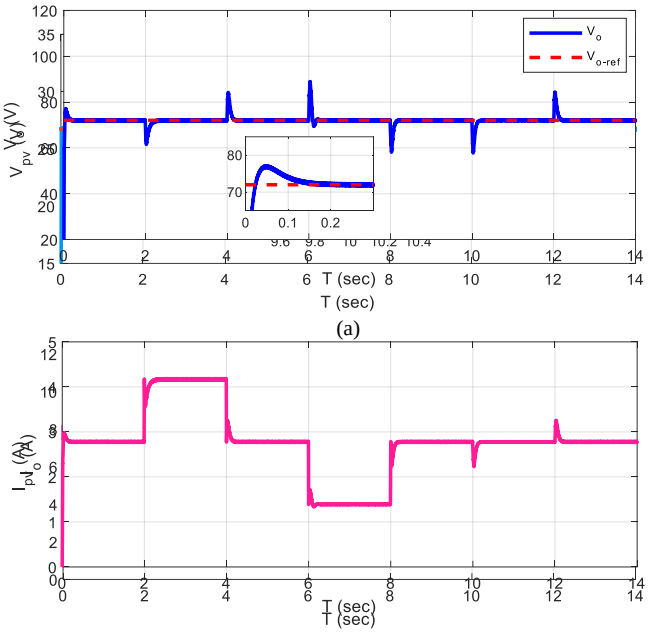

Fig. 4. Results of MPPT control. (a) PV output voltage, (b) PV output current

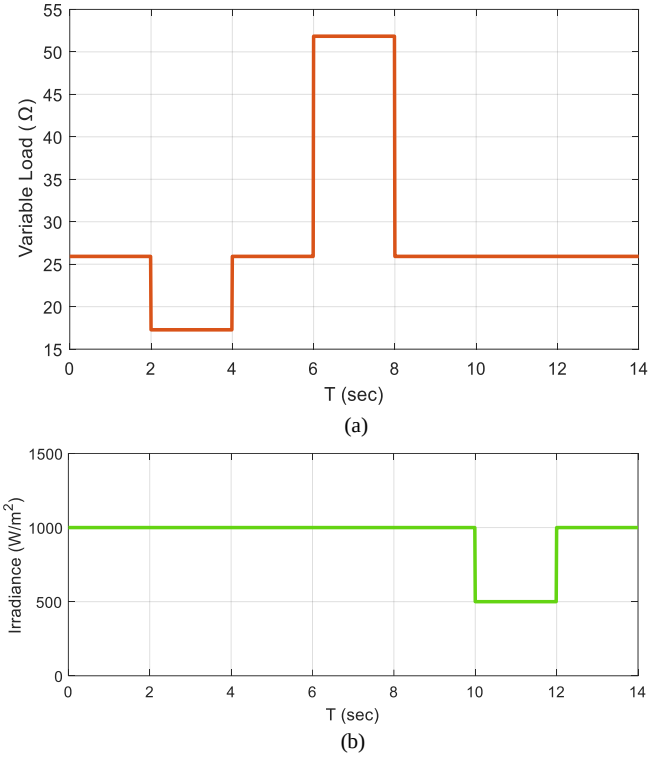

Fig. 5. Case studies. (a) Variable load profile, (b) Solar irradiation change

V. CONCLUSION

This paper proposed a nonlinear robust PI-SMC control method for voltage regulation and balanced demand response

Fig. 8. BESS Performance. (a) Battery current, (b) Battery voltage

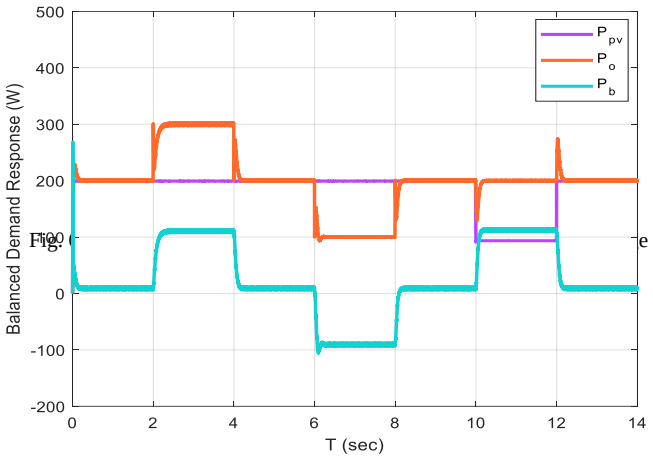

Fig. 6. e

of a standalone DC MG consisting of PV array and BESS in the presence of variable load and various solar irradiations. An MPP-based BSMC strategy is also investigated in order to reach the peak point and take out the maximum possible output of the solar panels. Moreover, BESS is becoming available to help the PV array in power delivery. The proposed control method discharges and charges the BESS to respond to the requested load power and store the excessive power respectively. The performance of the recommended control approach is proved by simulating the DC MG in the presence of demand variations and different irradiances. This strategy guarantees the robust voltage control of DC link efficiently with very small fluctuations and fast response. This model is also valid for long periods of time and for subscribers with higher consumption by adding additional PV modules and considering the accurate distribution of power among the solar PV and the BESS. In addition, the developed regulation method is easy to implement and guarantees the system stability.

Fig. 7. Balanced Demand Response

REFERENCES

[1] P. Singh, J. S. Lather, "Dynamic current sharing, voltage and SOC regulation for HESS based DC microgrid using CPISMC technique," Journal of Energy Storage, vol. 30, 101509, 2020.

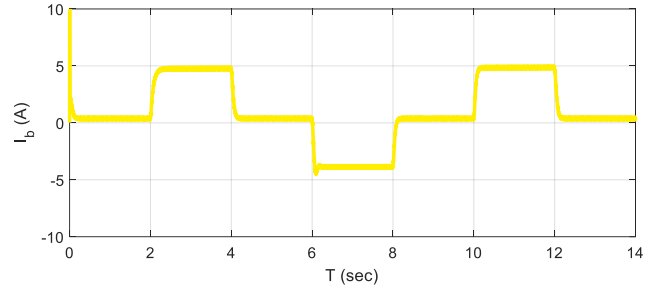

(a)

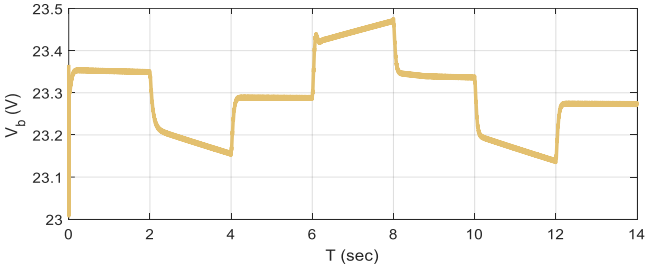

(b)

[2] K. Dahech, M. Allouche, T. Damak, F. Tadeo, "Backstepping sliding mode control for maximum power point tracking of a photovoltaic system," Electric Power Systems Research, vol. 143, pp. 182-188, 2017.

[3] V. Suresh, N. Pachauri, T. Vigneysh, "Decentralized control strategy for fuel cell/PV/BESS based microgrid using modified fractional order PI controller," International Journal of Hydrogen Energy, vol. 46, pp. 4417-4436, 2021.

[4] S. Vasantharaj, V. Indragandhi, V. Subramaniyaswamy, Y. Teekaraman, R. Kuppusamy, S. Nikolovski, "Efficient Control of DC Microgrid with Hybrid PV—Fuel Cell and Energy Storage Systems," Energies, vol. 14, 3234, 2021.

[5] S. K. Kollimalla, M. K. Mishra, A. Ukil, H. B. Gooi, "DC grid voltage regulation using new HESS control strategy," IEEE Trans. Sustain. Energy, vol. 8, pp. 772–781, 2017.

[6] Y. Zhang, W. Wei, "Model construction and energy management system of lithium battery, PV generator, hydrogen production unit and fuel cell in islanded AC microgrid," International Journal of Hydrogen Energy, vol. 45, pp. 16381-16397, 2020.

[7] R. Kumar, M. K. Pathak, "Distributed droop control of dc microgrid for improved voltage regulation and current sharing," IET Renewable Power Generation, vol. 14, pp. 2499–2506, 2020.

[8] M. Mokhtar, M. I. Marei, A. A. El-Sattar, "An adaptive droop control scheme for DC microgrids integrating sliding mode voltage and current controlled boost converters," Transactions on Smart Grid, vol. 10, pp. 1685–1693, 2018.

[9] S. Serna-Garcés, D. González Montoya, C. Ramos-Paja, "Control of a charger/discharger DC/DC converter with improved disturbance rejection for bus regulation," Energies, vol. 11, 594, 2018.

[10] D. Sattianadan, G. R. Prudhvi Kumar, R. Sridhar, Kuthuru Vishwas Reddy, Bhumireddy Sai Uday Reddy, Panga Mamatha, "Investigation of low voltage DC microgrid using sliding mode control," International Journal of Power Electronics and Drive System, vol. 11, pp. 2030-2037, 2020.

[11] Z. Karami, Q. Shafiee, Y. Khayat, M. Yaribeygi, T. Dragicevic, H. Bevrani, "Decentralized model predictive control of DC microgrids with constant power load," IEEE Journal of Emerging and Selected Topics in Power Electronics, vol. 9, pp. 451–460, 2020.

[12] S. Shoja Majidabad, A. Yazdani, "Paralleled DC-DC converters control using master-slave adaptive fuzzy backstepping techniques," Iranian Journal of Science and Technology, Transactions of Electrical Engineering, vol. 45, pp. 1343-1367. 2021.